IFAC

Selecting Uncertainty Structures in Identification for Robust Control with an Automotive Application

Tom Oomen* Okko Bosgra*

* *Eindhoven University of Technology, PO Box 513, Building WH, 5600 MB Eindhoven, The Netherlands.*

Abstract: The selection of uncertainty structures is an important aspect in system identification for robust control. The aim of this paper is to investigate the consequences for multivariable systems. Hereto, first a theoretical analysis is performed that establishes the connection between the associated model set and the robust control criterion. Second, an experimental case study for an automotive application confirms these connections. In addition, the experimental results provide new insights in the shape of associated model sets by using a novel validation procedure. Finally, the improved connections are confirmed through a robust controller synthesis. Both the theoretical and experimental results confirm that a recently developed robust-control-relevant uncertainty structure outperforms general dual-Youla-Kučera uncertainty, which in turn outperforms traditional uncertainty structures, including additive uncertainty.

1. INTRODUCTION

Attempts to connect system identification and robust control have led to many new results. First, it has led to approaches that consider deterministic assumptions on the noise, see Chen and Gu [2000]. Second, in a stochastic setting, connections between prediction error identification and robust control have been developed, and also the role of experimental conditions and experiment design have been investigated, see, e.g., Hjalmarsson [2005], Gevers [2005]. Third, iterative identification and control design approaches have been developed. Initially, these iterative approaches were based on nominal models, see Schrama [1992], Gevers [1993], and later extended in, e.g., de Callafon and Van den Hof [1997], to iterative identification and robust control design with guaranteed monotonic convergence.

An essential aspect in all these system identification approaches for robust control is the choice of uncertainty structure. Besides the use of parameter uncertainty, uncertainty structures in robust control have been further developed towards system identification. First, (inverse) additive and multiplicative uncertainty structures have been extended towards (normalized) coprime factor perturbations, see McFarlane and Glover [1990], to deal with closed-loop operation and to accommodate the control goal. These coprime factor-based uncertainty structures have been further refined towards dual-Youla uncertainty structures in, e.g., Anderson [1998], Douma and Van den Hof [2005], that improve the connection between identification and control by explicitly considering the closed-loop operation of the system. Recently, in Oomen and Bosgra [2012], these coprime factor-based uncertainty structures are further refined to explicitly connect the size of uncertainty and the control criterion. An essential advantage of the latter structure is that it provides an inherent scaling of the uncertainty channels that is essential for the nonconservative identification of model sets.

Although several uncertainty structures have been proposed in the area of system identification for robust control and several theoretical properties have been proved, at present a thorough comparison, especially taking into account experimental data, has not yet been established. In Jung et al. [2005], several uncertainty structures are experimentally compared on an automotive application. However, no explicit connection is established with identification and the results are not theoretically supported. In Douma and Van den Hof [2005], it is observed that if the nominal model and the weighting filters are allowed to vary, then many of these uncertainty structures can be explicitly related in terms of circular bounds in the frequency domain. However, such a frequency domain analysis does not explicitly address stability aspects, which is essential if $\mathcal{H}_\infty$-norm-bounded uncertainty is used. In addition, the present paper aims to analyze the consequences of uncertainty structures for a fixed nominal model.

The main contribution of this paper is to provide a theoretical and experimental comparison of uncertainty structures in robust control for a multivariable automotive application. To enable a fair comparison, the nominal model is pre-specified and identical experimental data is used for uncertainty modeling. To provide a solid theoretical framework to support the results, the identification and control criteria are connected using results from iterative identification and robust control (Sec. 2). Then, an overview of uncertainty structures in identification for robust control is provided and their properties are thoroughly analyzed from a theoretical perspective (Sec. 3). Next, these structures are experimentally compared from a system identification for robust control perspective (Sec. 4). Specifically, (i) the robust-control-relevant identification criterion, see Sec. 2, is evaluated; (ii) a novel visualization procedure, see Oomen et al. [2010a], is employed to generate Bode diagrams, providing insight in the characterization of control-relevant system properties; and (iii) the model sets are evaluated in their ability to deliver a high performance robust controller. Finally, the obtained results are discussed (Sec. 5).

2. PROBLEM FORMULATION

2.1 Setup

Throughout, the control criterion

$$\mathcal{J}(P, C) := \|WT(P, C)V\|_\infty \qquad (1)$$

is considered, where $W = \mathrm{diag}(W_y, W_u)$, $V = \mathrm{diag}(V_2, V_1)$, and $W, V, W^{-1}, V^{-1} \in \mathcal{RH}_\infty$ are user-defined weighting filters. In addition,

$$T(P,C) = \begin{bmatrix} P \\ I \end{bmatrix} (I + CP)^{-1} [C \; I],$$

where $T(P,C) : \begin{bmatrix} r_2 \\ r_1 \end{bmatrix} \mapsto \begin{bmatrix} y \\ u \end{bmatrix}$, see Fig. 1. The criterion (1) in conjunction with the four-block encompasses many relevant $\mathcal{H}_\infty$-design problems, including the loop-shaping approach in McFarlane and Glover [1990], and facilitates the synthesis of internally stabilizing controllers. The criterion (1) is formulated such that it is to be minimized for the true system P_o, i.e., $C^o = \arg\min_C \mathcal{J}(P_o, C)$.

The key idea in robust control is to consider a model set $\mathcal{P}$ such that

$$P_o \in \mathcal{P}. \qquad (2)$$

Consequently, the robust performance controller design

$$C^{\mathrm{RP}} = \arg\min_C \mathcal{J}_{\mathrm{WC}}(\mathcal{P}, C) \qquad (3)$$

$$\mathcal{J}_{\mathrm{WC}}(\mathcal{P}, C) := \sup_{P \in \mathcal{P}} \mathcal{J}(P, C),$$

is considered, leading to the performance guarantee

$$\mathcal{J}(P_o, C^{\mathrm{RP}}) \leq \mathcal{J}_{\mathrm{WC}}(\mathcal{P}, C^{\mathrm{RP}}). \qquad (4)$$

The main motivation for this paper stems from the observation that the resulting performance guarantee in (4) hinges on the shape and size of the model set $\mathcal{P}$. The key aspect in identification for robust control is to identify a model set $\mathcal{P}$ such that the bound (4) is as small as possible.

Throughout the paper, it is assumed that a nominal model $\hat{P}$ that approximates P_o is given. In addition, it is assumed that the model set $\mathcal{P}$ is constructed by connecting an $\mathcal{H}_\infty$-norm-bounded perturbation $\Delta_u \in \mathbf{\Delta}_u \subseteq \mathcal{RH}_\infty$ to the nominal model, i.e.,

$$\mathcal{P} = \left\{ P \big| P = \mathcal{F}_u(\hat{H}(\hat{P}), \Delta_u), \Delta_u \in \mathbf{\Delta}_u \right\}, \qquad (5)$$

where $\hat{H}(\hat{P})$ contains the nominal model $\hat{P}$ and the uncertainty structure, see Sec. 3 for details. The model uncertainty set

$$\mathbf{\Delta}_u := \{ \Delta_u | \|\Delta_u\|_\infty \leq \gamma \} \qquad (6)$$

is considered. It is assumed that $\mathbf{\Delta}_u$ contains multivariable operators with suitable dimensions. Furthermore, to facilitate the exposition and to enable a fair comparison, no additional weighting filters are assumed in (6). The aspect of weighting filters is further discussed in Sec. 5.

Notation. The pair $\{N, D\}$ is an RCF of P if i) $P = ND^{-1}$, ii) $N, D \in \mathcal{RH}_\infty$, and iii) $\exists X, Y \in \mathcal{RH}_\infty$ such that $XN + YD = I$. The pair $\{\tilde{N}, \tilde{D}\}$ is an LCF of P if $\{\tilde{N}^T, \tilde{D}^T\}$ is an RCF of P^T. In addition, the pair $\{\tilde{N}, \tilde{D}\}$ is an LCF with co-inner numerator of P if it is an LCF of P and, in addition, $\tilde{N}\tilde{N}^* = I$.

2.2 Problem formulation

The goal of this paper is to analyze the consequences of the choice of uncertainty structures in the identification of a multivariable system from experimental data in its ability to deliver a small upper bound in (4). An approach to address this problem is to compute C^{RP}, see (3), for various uncertainty structures and to compare the achieved robust performance in (4). However, the results of such an approach will highly depend on the considered application and do not provide insight in the underlying mechanism.

To provide an underlying theoretical framework for comparing model sets, use is made of the fact that identification and uncertainty modeling is generally performed in closed-loop with a given, non-optimal controller C^{exp} implemented
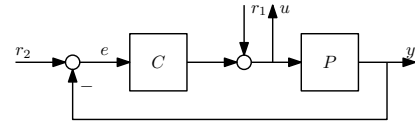

Fig. 1. Feedback interconnection.

to stabilize the system or to meet safety requirements. Next, suppose that a certain uncertainty structure is selected that leads to a model set $\mathcal{P}$ such that (2) is satisfied. Then, an approach to compare different model sets is to evaluate their worst-case performance

$$\mathcal{J}_{\mathrm{WC}}(\mathcal{P}, C^{\mathrm{exp}}). \qquad (7)$$

The motivation for considering (7) stems from the fact that (3) directly implies the bound

$$\mathcal{J}_{\mathrm{WC}}(\mathcal{P}, C^{\mathrm{RP}}) \leq \mathcal{J}_{\mathrm{WC}}(\mathcal{P}, C^{\mathrm{exp}}). \qquad (8)$$

Thus, given two model sets $\mathcal{P}^1$ and $\mathcal{P}^2$, if $\mathcal{J}_{\mathrm{WC}}(\mathcal{P}^1, C^{\mathrm{exp}}) < \mathcal{J}_{\mathrm{WC}}(\mathcal{P}^2, C^{\mathrm{exp}})$, then (8) implies that $\mathcal{P}^1$ has a tighter upper bound compared to $\mathcal{P}^2$ regarding the resulting robust performance. Note that this upper bound does not imply an ordering in the robust performance as is achieved by $C^{\mathrm{RP}}(\mathcal{P}^1)$ and $C^{\mathrm{RP}}(\mathcal{P}^2)$. However, extensive experimental results, as is also supported by the results in Sec. 4, reveal that $\mathcal{J}_{\mathrm{WC}}(\mathcal{P}^1, C^{\mathrm{exp}}) < \mathcal{J}_{\mathrm{WC}}(\mathcal{P}^2, C^{\mathrm{exp}})$ typically leads to $\mathcal{J}_{\mathrm{WC}}(\mathcal{P}^1, C^{\mathrm{RP}}(\mathcal{P}^1)) < \mathcal{J}_{\mathrm{WC}}(\mathcal{P}^2, C^{\mathrm{RP}}(\mathcal{P}^2))$.

Furthermore, the minimization of (7) over $\mathcal{P}$, subject to (2), is at the heart of iterative identification and robust control approaches, including de Callafon and Van den Hof [1997], Oomen and Bosgra [2012]. An important advantage of the criterion (7) is that the robust control design (3) and identification problem (7) may be solved alternately, leading to a monotonously converging iterative procedure Bayard et al. [1992]. In this paper, the criterion (7) is adopted to evaluate the consequences of the choice of uncertainty structure, see (5), for a pre-specified model $\hat{P}$.

As a final aspect, the experimental conditions directly influence the size of model uncertainty. To enable a fair comparison, the same data set is used for different uncertainty structures. It is emphasized that the results in this paper are largely independent of the employed uncertainty modeling approach.

Next, several uncertainty structures are surveyed and evaluated theoretically in their ability to minimize (7).

3. IDENTIFICATION-RELATED UNCERTAINTY STRUCTURES FOR ROBUST CONTROL

In this section, several uncertainty structures that arise in system identification for robust control are presented and analyzed. Each of these uncertainty structures gives rise to an uncertain model set that can be cast as an LFT, see (5). Hence, the performance of the model set, interconnected with C^{exp} follows from the construction of a generalized plant, see [Skogestad and Postlethwaite, 2005, Sec. 3.8]

$$\mathcal{J}_{\mathrm{WC}}(\mathcal{P}, C^{\mathrm{exp}}) = \sup_{\Delta \in \mathbf{\Delta}_u} \|\mathcal{F}_u(\hat{M}, \Delta_u)\|_\infty, \qquad (9)$$

where

$$\hat{M}(\hat{H}, C^{\mathrm{exp}}) = \left[\begin{array}{c|c} \hat{M}_{11} & \hat{M}_{12} \\ \hline \hat{M}_{21} & \hat{M}_{22} \end{array} \right]. \qquad (10)$$

The matrix $\hat{M}$ in (10) depends on the uncertainty structure $\hat{H}$ as chosen in (5). In the forthcoming sections, several uncertainty structures in identification for robust control are evaluated in their (i) capability to satisfy (2), and (ii) associated worst-case performance in (7) and (9).

3.1 Traditional uncertainty structures for robust control

Commonly, (inverse) additive and (inverse) multiplicative uncertainty structures are used in robust controller designs. Firstly, consider a multivariable model set based on additive uncertainty that is given by

$$\mathcal{P}^{\mathrm{ADD}} := \{P | P = \hat{P} + \Delta_u, \Delta_u \in \boldsymbol{\Delta}_u\}, \qquad (11)$$

where all considered systems have appropriate dimensions. The corresponding $\hat{H}(\hat{P})$ is given by

$$\hat{H}^{\mathrm{ADD}} = \begin{bmatrix} 0 & I \\ I & \hat{P} \end{bmatrix},$$

whereas direct computations reveal that the worst-case performance in (9) is given by

$$\mathcal{J}_{\mathrm{WC}}(\mathcal{P}^{\mathrm{ADD}}, C^{\mathrm{exp}}) = \sup_{\Delta_u \in \boldsymbol{\Delta}_u} \left\| \hat{M}_{22}^{\mathrm{ADD}} + \right. $$
$$\left. \hat{M}_{21}^{\mathrm{ADD}} \Delta_u (I - \hat{M}_{11}^{\mathrm{ADD}} \Delta_u)^{-1} \hat{M}_{12}^{\mathrm{ADD}} \right\|_\infty, \qquad (12)$$

for a certain $\hat{M}^{\mathrm{ADD}}$, see (10), with in general $\hat{M}_{11}^{\mathrm{ADD}} \neq 0$. Hence, the worst-case performance associated with $\mathcal{P}^{\mathrm{ADD}}$, see (12), is thus arbitrary and may in fact become unbounded for a bounded $\Delta_u \in \boldsymbol{\Delta}_u$. From this perspective, such additive uncertainty structures do not provide a useful bound in (8). In fact, similar results hold for all uncertainty structures in [Zhou et al., 1996, Table 9.1], including (inverse) multiplicative structures.

Besides the absence of a finite upper bound in (8), a key shortcoming of additive and multiplicative uncertainty structures involves the fact that the constraint (2) may not hold if such uncertainty structures are used. For instance, from (11) it is immediate that the additive uncertainty structure cannot deal with uncertain *unstable* poles of $\hat{P}$, e.g., if P_o is unstable, then for a stable model $\hat{P}$, it holds that $\hat{P} + \Delta_u \in \mathcal{RH}_\infty$, hence (2) cannot be satisfied.

3.2 Towards coprime-factor based uncertainty structures

To ensure that the constraint in (2) holds for a certain $\Delta_u \in \boldsymbol{\Delta}_u \subseteq \mathcal{H}_\infty$, perturbations on coprime factors can be considered, i.e.,

$$\mathcal{P}^{\mathrm{CF}} = \{P | P = (\hat{N} + \Delta_N)(\hat{D} + \Delta_D)^{-1}, \| \begin{bmatrix} \Delta_N^T & \Delta_D^T \end{bmatrix}^T \|_\infty \leq \gamma\}, \quad (13)$$

where $\{\hat{N}, \hat{D}\}$ is an RCF of $\hat{P}$. In fact, certain coprime factorizations have a close connection to robustness in the graph and (ν-) gap metric, see Georgiou and Smith [1990] and Vinnicombe [2001]. Although these guarantee that the constraint (2) is satisfied for at least one $\Delta_u \in \mathcal{RH}_\infty$, such uncertainty structures lead to the general worst-case performance expression in (12). This results follows immediately since if $\hat{P} \in \mathcal{RH}_\infty$, then $\{\hat{P}, I\}$ is an RCF of $\hat{P}$. Hence, the coprime factor uncertainty structure encompasses additive uncertainty as a special case. Hence, in general these coprime factor perturbations do not necessarily lead to finite bounds in the sense of (8).

3.3 Dual-Youla-Kučera uncertainty structures

To ensure that both the constraint (2) holds and that the bound in (8) is finite, the dual-Youla-Kučera uncertainty structure has been considered in, e.g., Anderson [1998], Douma and Van den Hof [2005]. Specifically,

$$\mathcal{P}^{\mathrm{DY}} := \left\{ P | P = \left(\hat{N} + D_c \Delta_u \right) \left(\hat{D} - N_c \Delta_u \right)^{-1}, \Delta_u \in \boldsymbol{\Delta}_u \right\},$$
$$(14)$$

where the pairs $\{\hat{N}, \hat{D}\}$ and $\{N_c, D_c\}$ are *any* RCF of $\hat{P}$ and C^{exp}, respectively. The key point is that P_o by definition corresponds to a $\Delta_u \in \mathcal{H}_\infty$. The model set $\mathcal{P}^{\mathrm{DY}}$ leads to

$$\hat{H}^{\mathrm{DY}} = \left[\begin{array}{c|c} \hat{D}^{-1} N_c & \hat{D}^{-1} \\ \hline D_c + \hat{P} N_c & \hat{P} \end{array} \right]$$

and

$$\hat{M}^{\mathrm{DY}}(\hat{P}, C^{\mathrm{exp}}) = \left[\begin{array}{c|c} 0 & (\hat{D} + C^{\mathrm{exp}} \hat{N})^{-1} \begin{bmatrix} C^{\mathrm{exp}} & I \end{bmatrix} V \\ \hline W \begin{bmatrix} D_c \\ -N_c \end{bmatrix} & W T(\hat{P}, C^{\mathrm{exp}}) V \end{array} \right]$$
$$(15)$$

Interestingly, (15) can be written as

$$\mathcal{J}_{\mathrm{WC}}(\mathcal{P}^{\mathrm{DY}}, C^{\mathrm{exp}}) = \sup_{\Delta_u \in \boldsymbol{\Delta}_u} \left\| \hat{M}_{22} + \hat{M}_{21} \Delta_u \hat{M}_{12} \right\|_\infty, \qquad (16)$$

which is an affine function of Δ_u and hence bounded for all $\Delta_u \in \boldsymbol{\Delta}_u$. However, it is emphasized that $\hat{M}_{12}$ and $\hat{M}_{21}$ in (16) are frequency-dependent and multivariable transfer function matrices. Consequently, the bound in (16) and (8) is finite but in general arbitrary. Thus, the dual-Youla-Kučera model uncertainty structure, which connects the perturbations on the coprime factors in (13) through the controller C^{exp}, is especially useful from a robust stability perspective, since it excludes candidate models that are not stabilized by C^{exp}.

3.4 Uncertainty structures for achieving robust performance

In Oomen and Bosgra [2012], a new model uncertainty structure has been presented that has distinct advantages from a robust performance perspective. A key ingredient of this uncertainty structure is a new coprime factorization that arises in a novel connection between control-relevant identification of nominal models and coprime factor identification, extending and providing new insights in earlier results, including Schrama [1992]. This robust-control-relevant coprime factorization of $\hat{P}$ is given by

$$\begin{bmatrix} \hat{N}^{\mathrm{RCR}} \\ \hat{D}^{\mathrm{RCR}} \end{bmatrix} = \begin{bmatrix} \hat{P} \\ I \end{bmatrix} (\tilde{D}_e + \tilde{N}_{e,2} V_2^{-1} \hat{P})^{-1},$$

where the pair $([\tilde{N}_{e,2} \ \tilde{N}_{e,1}], \tilde{D}_e)$ is an LCF with co-inner numerator of C^{exp}, see Zhou et al. [1996]. A second ingredient is a certain (W_u, W_y)-normalized RCF, see Oomen and Bosgra [2012]. Specifically, the pair $\{N_c^W, D_c^W\}$ is a (W_u, W_y)-normalized RCF of C if it is an RCR and, in addition, $(W_u N_c)^* W_u N_c + (W_y D_c)^* W_y D_c = I$.

Next, by employing the specific robust-control-relevant coprime factorization $\{\hat{N}^{\mathrm{RCR}}, \hat{D}^{\mathrm{RCR}}\}$ of $\hat{P}$ in conjunction with a (W_u, W_y)-normalized RCF of C^{exp}, and equation (14), a new model set is obtained:

$$\mathcal{P}^{\mathrm{RCR}} := \left\{ P \middle| P = \left(\hat{N}^{\mathrm{RCR}} + D_c^W \Delta_u \right) \left(\hat{D}^{\mathrm{RCR}} - N_c^W \Delta_u \right)^{-1}, \Delta_u \in \boldsymbol{\Delta}_u \right\},$$
$$(17)$$

The robust-control-relevant model set $\mathcal{P}^{\mathrm{RCR}}$ leads to

$$\hat{H}^{\mathrm{RCR}} = \left[\begin{array}{c|c} (\hat{D}^{\mathrm{RCR}})^{-1} N_c^W & (\hat{D}^{\mathrm{RCR}})^{-1} \\ \hline D_c^W + \hat{P} N_c^W & \hat{P} \end{array} \right]$$

and

$$\hat{M}^{\mathrm{RCR}}(\hat{P}, C^{\mathrm{exp}}) = \left[\begin{array}{c|c} 0 & (\hat{D}^{\mathrm{RCR}} + C^{\mathrm{exp}} \hat{N}^{\mathrm{RCR}})^{-1} \begin{bmatrix} C^{\mathrm{exp}} & I \end{bmatrix} V \\ \hline W \begin{bmatrix} D_c^W \\ -N_c^W \end{bmatrix} & W T(\hat{P}, C^{\mathrm{exp}}) V \end{array} \right]$$
$$(18)$$

The result (18) leads to a significantly stronger result when compared to (16). Specifically, a main result of Oomen and Bosgra [2012] reveals that

$$\mathcal{J}_{\text{WC}}(\mathcal{P}^{\text{RCR}}, C^{\text{exp}}) \le \|\hat{M}_{22}^{\text{RCR}}\|_\infty + \sup_{\Delta_u \in \boldsymbol{\Delta}_u} \|\Delta_u\|_\infty \qquad (19)$$
$$= \mathcal{J}(\hat{P}, C^{\text{exp}}) + \gamma,$$

where γ is defined in (6). The robust-control-relevant model uncertainty structure associated with $\mathcal{P}^{\text{RCR}}$ connects the size of model uncertainty and the control criterion. This has significant advantages when compared to alternative model uncertainty structures, including $\mathcal{P}^{\text{ADD}}$ and $\mathcal{P}^{\text{RCR}}$. Firstly, the robust-control-relevant model uncertainty structure introduces an appropriate frequency scaling of the model uncertainty channels, hence $\hat{M}_{12}$ and $\hat{M}_{21}$ do not appear in (19). Secondly, the robust-control-relevant model uncertainty structure introduces an appropriate scaling of the model uncertainty channels for multivariable systems by scaling these with respect to the control criterion. Indeed, the scaling of different inputs and outputs is considered important in control system design, see, e.g., [Skogestad and Postlethwaite, 2005, Sec. 1.4]. The appropriate scaling enables the nonconservative use of unstructured model uncertainty, which has significant advantages for certain uncertainty modeling procedures, see, e.g., Toker and Chen [1998], and robust controller synthesis.

4. EXPERIMENTAL COMPARISON FOR AN AUTOMOTIVE APPLICATION

Although the theoretical analysis in Sec. 3 provides an ordering of uncertainty structures in the sense of (7), it has not yet been established whether the differences between (12), (16), and (19) are significant for an actual experimental application. In addition, it remains to be shown whether the ordering of uncertainty structures implied by (7) leads to a similar ordering in terms of achieved robust performance. These aspects are investigated in this section.

4.1 Experimental CVT setup

The considered continuously variable transmission (CVT) system is depicted in Fig. 2. The CVT provides a continuous range of transmission ratios, which enables optimal engine operating conditions in cars.

For optimal CVT operation, it is of crucial importance that certain reference pressures are achieved by the closed-loop system, see Oomen et al. [2010b], van der Meulen et al. [2012] for details. In view of the signals in Fig. 1, the error

$$e = \begin{bmatrix} e^p \\ e^s \end{bmatrix} = \begin{bmatrix} r_2^p - y^p \\ r_2^s - y^s \end{bmatrix}$$

should be small in some appropriate sense. Hereto, the measured variables y and manipulated variables u are given by

$$y = \begin{bmatrix} y_p \\ y_s \end{bmatrix} = \begin{bmatrix} p_p \\ p_s \end{bmatrix}, \quad u = \begin{bmatrix} u_p \\ u_s \end{bmatrix} = \begin{bmatrix} V_p \\ V_s \end{bmatrix},$$

respectively. Here, V_p and V_s are the voltages corresponding to the primary and secondary servo valve, respectively.

In this paper, weighting filters W and V, see (1), an experimental controller C^{exp}, see Sec. 2.2, and a nominal model $\hat{P}$, see (5), are fixed. Specifically, use is made of the loop-shaping based weighting filters W and V in Oomen et al. [2010b] that are aimed at enhancing CVT performance. Specifically, the weighting filters aim at a bandwidth of 6 [Hz]. In addition, the experimental controller C^{exp} in Oomen et al. [2010b] is employed. Finally, in Oomen et al. [2010b], the weighting filters W and V and controller C^{exp} is used to identify a control-relevant
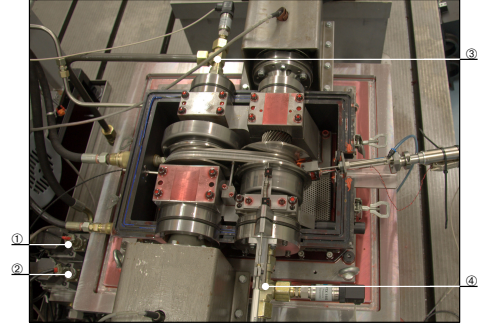

Fig. 2. Photograph of the experimental CVT system, where ①: primary servo valve V_p, ②: secondary servo valve V_s, ③: pressure measurement p_p at primary hydraulic cilinder, ④: pressure measurement p_s at secondary hydraulic cilinder.

parametric model $\hat{P}$, which is internally structured as a robust-control-relevant coprime factorization, i.e., $\hat{P} = \hat{N}\hat{D}^{-1}$, see also Sec. 3.1. Hence, by definition, $\hat{N}, \hat{D} \in \mathcal{RH}_\infty^{2\times2}$. In addition, for the specific control-relevant model of the CVT, it turns out that $\hat{P} = \hat{N}\hat{D}^{-1} \in \mathcal{RH}_\infty^{2\times2}$. It is emphasized that there are no *a priori* guarantees with respect to open-loop stability of the model $\hat{P}$, since it is estimated in a control-relevant manner that enforces closed-loop stability of the interconnection of $\hat{P}$ and C^{exp}.

4.2 Model uncertainty structures

Three important model structures, in particular, (11), (14), and (17), are compared for clarity of exposition. As is explained in Sec. 3.1, an additive structure can be used in this application, since the nominal model does not contain any open-loop unstable poles, see also [Zhou et al., 1996, Table 9.1]. It is emphasized that this is not possible in general, since additive uncertainty cannot guarantee that the bound in (2) is guaranteed for a finite γ in (6), as is exemplified in Sec. 3.1. In general, the minimum norm-bound γ to satisfy (2) is different for each uncertainty structure in $\hat{H}$. Note that unstructured perturbation models, i.e., $\Delta_u \in \mathcal{RH}_\infty^{2\times2}$, are considered in all cases without any additional weighting filters to facilitate the interpretation.

Firstly, the additive uncertainty structure can directly be considered using the result in (11). Secondly, RCFs of $\hat{P}$ and C^{exp} are required to construct the dual-Youla-Kučera uncertainty structure in (14). Hereto, observe that $\hat{P} \in \mathcal{RH}_\infty$, hence the pair $\{\hat{P}, I\}$ clearly is an RCF of $\hat{P}$. Since the controller C^{exp} contains a pure integrator, $C^{\text{exp}} \ne \mathcal{RH}_\infty$. Hence, C^{exp} cannot be used directly as a coprime factor. To resolve this, two closed-loop transfer functions are postulated as a coprime factorization for C^{exp}, i.e.,

$$\begin{bmatrix} N_c \\ D_c \end{bmatrix} = \begin{bmatrix} C^{\text{exp}} \\ I \end{bmatrix} (I + \hat{P}C^{\text{exp}})^{-1} \in \mathcal{RH}_\infty. \qquad (20)$$

Clearly, by setting $X = \hat{P}$, $Y = I$, it appears that the Bézout identity $XN + YD = I$ is satisfied. Hence, the pair $\{N_c, D_c\}$ in (20) indeed is an RCF of C^{exp}. Consequently, all RCFs of C^{exp} are generated by $\{N_c Q_c, D_c Q_c\}$, $Q_c, Q_c^{-1} \in \mathcal{RH}_\infty^{2\times2}$. Thirdly, the robust-control-relevant model uncertainty structure in (19) is constructed by employing the robust-control-relevant coprime factorization $\hat{P} = \hat{N}\hat{D}^{-1}$ as described in Sec. 4.1 in conjunction with a (W_u, W_y)-normalized RCF of C^{exp}, which is computed using the state-space results in Oomen and Bosgra [2012].

Table 1. Comparison of uncertainty structures.

	$\mathcal{P}^{\mathrm{ADD}}$	$\mathcal{P}^{\mathrm{DY}}$	$\mathcal{P}^{\mathrm{RCR}}$
Open-loop uncertain model set	(11)	(14)	(17)
Closed-loop performance bound	(12)	(16)	(19)
γ	1.73	0.55	0.60
$\mathcal{J}(\hat{P}, C^{\mathrm{exp}})$	6.14	6.14	6.14
$\mathcal{J}_{\mathrm{WC}}(\mathcal{P}, C^{\mathrm{exp}})$	∞	11.06	6.73
$\min_C \mathcal{J}_{\mathrm{WC}}(\mathcal{P}, C)$	3.63	3.20	2.50

The required bound to satisfy (2) is determined individually for each uncertainty structure. A validation-based uncertainty modeling procedure, see Smith and Doyle [1992] and Oomen and Bosgra [2009], is employed. This approach leads to the minimum norm-bound γ such that the model set is consistent with the data, i.e., such that there are no indications that, given the data, the constraint (2) does not hold. The resulting values of γ are given in Table 1. Note that a static overbound is considered here, instead of a possibly frequency-dependent function, see Sec. 5.

4.3 Analysis of identification-related model sets

Skewed-μ analysis   The criterion in (8), i.e., $\mathcal{J}_{\mathrm{WC}}(\mathcal{P}, C^{\mathrm{exp}})$ is adopted to compare the various model sets. Hereto, skewed-μ analysis is invoked. The pursued approach is to perform a sequence of μ-analysis problems, see also Fan and Tits [1992]. Although in general these computations involve upper bounds, the results in this paper are exact since the considered perturbation structure is μ-simple.

Firstly, it is observed that $\mathcal{J}_{\mathrm{WC}}(\mathcal{P}^{\mathrm{ADD}}, C^{\mathrm{exp}})$ is unbounded. Hence, the model set contains at least one candidate model that is not stabilized by C^{exp}. By virtue of (8), the model set $\mathcal{P}^{\mathrm{ADD}}$ does not seem to be a good candidate for robust control design. Secondly, the controller C^{exp} stabilizes all candidate models in $\mathcal{P}^{\mathrm{DY}}$, which is also reflected by the affine function in (16), hence $\mathcal{J}_{\mathrm{WC}}(\mathcal{P}^{\mathrm{DY}}, C^{\mathrm{exp}})$ indeed is bounded. Specifically, the model set $\mathcal{P}^{\mathrm{DY}}$ leads to a worst-case performance $\mathcal{J}_{\mathrm{WC}}(\mathcal{P}^{\mathrm{DY}}, C^{\mathrm{exp}}) = 11.06$. It is emphasized that this value is arbitrarily large, since it depends on the transfer function matrices $\hat{M}_{12}$ and $\hat{M}_{21}$ in (16), which in turn depend on the arbitrarily chosen coprime factorizations of $\hat{P}$ and C^{exp} in Sec. 4.2. By virtue of (8), the dual-Youla-Kučera model set has advantageous properties when compared to the additive model set $\mathcal{P}^{\mathrm{ADD}}$. Thirdly, the robust-control-relevant model set $\mathcal{P}^{\mathrm{RCR}}$ achieves the smallest worst-case performance, i.e., $\mathcal{J}_{\mathrm{WC}}(\mathcal{P}^{\mathrm{RCR}}, C^{\mathrm{exp}}) = 6.73$. In addition, these results confirm that the bound (19) holds and is tight.

Visualization   To further interpret these results, the model sets $\mathcal{P}^{\mathrm{ADD}}$ and $\mathcal{P}^{\mathrm{RCR}}$ are depicted in Bode diagrams using the novel visualization procedure that is presented in Oomen et al. [2010a]. Similar results are obtained for $\mathcal{P}^{\mathrm{DY}}$, however these results are omitted due to space limitations.

Firstly, it is observed that the additive model set $\mathcal{P}^{\mathrm{ADD}}$ leads to a relatively small uncertainty in at low frequencies. In contrast, the robust-control-relevant model set $\mathcal{P}^{\mathrm{RCR}}$ leads to an extremely large uncertainty at low frequencies.

Secondly, around the desired bandwidth of 6 [Hz], see Sec. 4.1, the robust-control-relevant model set $\mathcal{P}^{\mathrm{RCR}}$ is very accurate and hence the uncertainty in all the open-loop transfer functions is small. In contrast, the additive model set $\mathcal{P}^{\mathrm{ADD}}$ is significantly more uncertain in this frequency range, especially when considering the elements P_{22}, P_{21}, and P_{12}. Hence, the uncertainty associated with
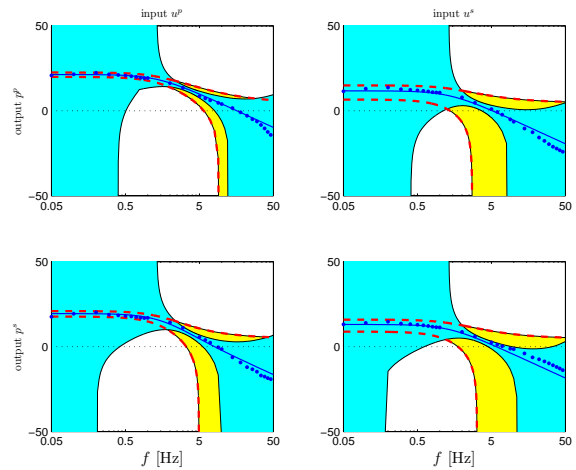

Fig. 3. Nominal model $\hat{P}$ (solid blue), frequency response function estimate $\widetilde{P}_o(\omega_i), \omega_i \in \Omega^{\mathrm{id}}$ (blue dots), and model set $\mathcal{P}^{\mathrm{RCR}}$ (cyan) and $\mathcal{P}^{\mathrm{ADD}}$ (yellow, red dashed).

the additive model set $\mathcal{P}^{\mathrm{ADD}}$ is not only significantly larger, but also seems to suffer from an inappropriate scaling of the uncertainty channels. In contrast, the model set $\mathcal{P}^{\mathrm{RCR}}$ leads to an optimal scaling of the uncertainty channels from a control perspective, see (19).

Thirdly, at the higher frequency ranges, both the model sets $\mathcal{P}^{\mathrm{RCR}}$ and $\mathcal{P}^{\mathrm{ADD}}$ exhibit a large uncertainty. An explanation is that in the case of $\mathcal{P}^{\mathrm{RCR}}$, the model quality at the higher frequency ranges typically does not affect the control performance [McFarlane and Glover, 1990]. In case of $\mathcal{P}^{\mathrm{ADD}}$, the gain of the open-loop model $\hat{P}$ is significantly smaller at higher frequencies, hence (11) implies that the model uncertainty has a larger relative effect.

Robust controller synthesis   The model sets $\mathcal{P}$ and $\mathcal{P}^{\mathrm{ADD}}$ are further investigated though a robust controller synthesis. Note that the bound in (8) holds for each of the model sets in Sec. 4.2. However, no explicit statements can be made regarding the ordering of the resulting controllers in terms of worst-case performance.

Firstly, consider $C^{\mathrm{RCR}} = \arg\min_C \mathcal{J}_{\mathrm{WC}}(\mathcal{P}^{\mathrm{RCR}}, C)$ that provides the performance guarantees

$$\mathcal{J}(P_o, C^{\mathrm{RCR}}) \leq \mathcal{J}_{\mathrm{WC}}(\mathcal{P}^{\mathrm{RCR}}, C^{\mathrm{RCR}}) \leq \mathcal{J}_{\mathrm{WC}}(\mathcal{P}^{\mathrm{RCR}}, C^{\mathrm{exp}}) = 6.73.$$

Indeed, the controller C^{RCR} leads to $\mathcal{J}_{\mathrm{WC}}(\mathcal{P}^{\mathrm{RCR}}, C^{\mathrm{RCR}}) = 2.50$ Secondly, recall that the additive model set $\mathcal{P}^{\mathrm{ADD}}$ leads to an infinite worst-case when evaluated for C^{exp}, see Table 1, since the model set is not robustly stable under closed-loop with C^{exp} implemented. Since the model set $\mathcal{P}^{\mathrm{ADD}}$ is open-loop stable, clearly a controller exists that simultaneously stabilizes all candidate models in $\mathcal{P}^{\mathrm{ADD}}$. In fact, $C = 0$ is such a stabilizing controller. Hence, $C^{\mathrm{ADD}} = \arg\min_C \mathcal{J}_{\mathrm{WC}}(\mathcal{P}^{\mathrm{ADD}}, C)$ always leads to an bounded worst-case performance. However, the worst-case performance is arbitrary, since $\mathcal{J}_{\mathrm{WC}}(\mathcal{P}^{\mathrm{ADD}}, C^{\mathrm{exp}})$ is unbounded. Analysis of the optimal controller C^{ADD} leads to $\mathcal{J}_{\mathrm{WC}}(\mathcal{P}^{\mathrm{ADD}}, C^{\mathrm{ADD}}) = 3.63$. For this specific situation, the controller C^{ADD} achieves a reasonably good performance. It is emphasized that this is to a large extent attributed to the favorable scaling and specific properties of the open-loop model $\hat{P}$. In general, $\mathcal{J}_{\mathrm{WC}}(\mathcal{P}^{\mathrm{ADD}}, C^{\mathrm{ADD}})$ may be arbitrarily worse than $\mathcal{J}_{\mathrm{WC}}(\mathcal{P}, C^{\mathrm{exp}})$.
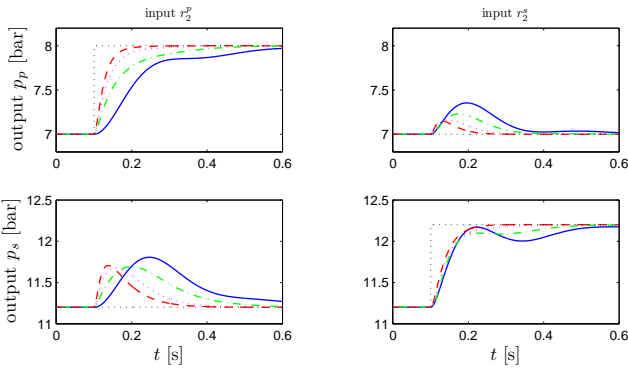
Fig. 4. Closed-loop step responses ($r_2 \mapsto y$): initial controller C^{exp} (solid blue), optimal robust controller C^{RCR} (dashed red), C^{ADD} (dash-dotted green), and C^{DY} (dotted).

Thirdly, the controller $C^{\mathrm{DY}} = \arg\min_C \mathcal{J}_{\mathrm{WC}}(\mathcal{P}^{\mathrm{DY}}, C)$ is computed, leading to $\mathcal{J}_{\mathrm{WC}}(\mathcal{P}^{\mathrm{DY}}, C^{\mathrm{DY}}) = 3.20$. Interestingly, the ordering of $\mathcal{P}^{\mathrm{ADD}}$, $\mathcal{P}^{\mathrm{DY}}$, and $\mathcal{P}^{\mathrm{RCR}}$ in terms of $\mathcal{J}_{\mathrm{WC}}(\mathcal{P}, C^{\mathrm{exp}})$, i.e.,

$$\mathcal{J}_{\mathrm{WC}}(\mathcal{P}^{\mathrm{ADD}}, C^{\mathrm{exp}}) \geq \mathcal{J}_{\mathrm{WC}}(\mathcal{P}^{\mathrm{DY}}, C^{\mathrm{exp}}) \geq \mathcal{J}_{\mathrm{WC}}(\mathcal{P}^{\mathrm{RCR}}, C^{\mathrm{exp}}) \quad (21)$$

corresponds to an identical ordering in terms of the optimal robust controllers C^{ADD}, C^{DY}, and C^{RCR} that are based on these model sets, i.e.,

$$\mathcal{J}_{\mathrm{WC}}(\mathcal{P}^{\mathrm{ADD}}, C^{\mathrm{ADD}}) \geq \mathcal{J}_{\mathrm{WC}}(\mathcal{P}^{\mathrm{DY}}, C^{\mathrm{DY}}) \geq \mathcal{J}_{\mathrm{WC}}(\mathcal{P}^{\mathrm{RCR}}, C^{\mathrm{RCR}}). \quad (22)$$

It is emphasized that the ordering in (21) and (22) typically arises in subsequent identification and robust controller synthesis, but is not guaranteed.

Finally, the resulting controllers are implemented on the nominal model $\hat{P}$, see Sec. 4.1. The resulting step responses in Fig. 4 confirm that a reduced worst-case performance leads to a faster response in terms of settling time and less interaction, hence improved performance.

5. CONCLUSION AND DISCUSSION

In this paper, uncertainty structures in identification for robust control are thoroughly and experimentally compared. Theoretical and experimental results confirm that (i) the dual-Youla-Kučera uncertainty structure has significant advantages over common uncertainty structures, including additive uncertainty; and (ii) recently developed robust-control-relevant uncertainty structures, see Oomen and Bosgra [2012], have significant advantages compared to general dual-Youla-Kučera uncertainty structures and hence also compared to traditional uncertainty structures. Although not explicitly investigated in the present paper, commonly used *normalized* coprime factorizations generally do not seem to have advantageous properties in identification for robust control, see Oomen and Bosgra [2012] for details. Furthermore, the correspondence between the partial ordering in (21) and (22) underpins the relevance of the robust-control-relevant identification criterion (7) and supports its use in an (iterative) identification and robust control design approach.

The results in this paper have been restricted to model uncertainty without commonly used weighting filters. Indeed, it is common practice to consider $\boldsymbol{\Delta}_u^W :=$ $\{\Delta_u | \|W_\Delta \Delta_u V_\Delta\|_\infty \leq \gamma\}$ instead of (6), where W_Δ, V_Δ, W_Δ^{-1}, V_Δ^{-1}. These weighting filters W_Δ and V_Δ can be used to mitigate the conservatism in, e.g., additive and dual-Youla-Kučera uncertainty structures. However, the selection of these weights is not straightforward, especially for multivariable systems. This is evidenced by the use

of highly structured perturbation models in, e.g., van de Wal et al. [2002] and de Callafon and Van den Hof [2001] for additive and dual-Youla-Kučera uncertainty structures, respectively. In contrast to (6), such an approach leads to model validation and robust controller synthesis procedures that are proven to be computationally hard, see Toker and Chen [1998]. In this respect, the robust-control-relevant uncertainty structure, see (17), can be considered as an inherent optimal selection of W_Δ and V_Δ in view of the control goal. Indeed, recently in van Herpen et al. [2011], it is shown that (6) leads to optimal results in view of (7).

In future research, it is of interest to compare the presented results to other uncertainty structures, including those that represent uncertainty in a parametric space.

REFERENCES

B. D. O. Anderson. From Youla-Kucera to identification, adaptive and nonlinear control. *Automatica*, 34(12):1485–1506, 1998.

D. S. Bayard, Y. Yam, and E. Mettler. A criterion for joint optimization of identification and robust control. *IEEE Trans. Automat. Contr.*, 37(7):986–991, 1992.

R. A. de Callafon and P. M. J. Van den Hof. Suboptimal feedback control by a scheme of iterative identification and control design. *Math. Mod. Syst.*, 3 (1):77–101, 1997.

R. A. de Callafon and P. M. J. Van den Hof. Multivariable feedback relevant system identification of a wafer stepper system. *IEEE Trans. Contr. Syst. Techn.*, 9(2):381–390, 2001.

J. Chen and G. Gu. *Control-Oriented System Identification: An $\mathcal{H}_\infty$ Approach*. John Wiley & Sons, New York, NY, USA, 2000.

S. G. Douma and P. M. J. Van den Hof. Relations between uncertainty structures in identification for robust control. *Automatica*, 41:439–457, 2005.

M. K. H. Fan and A. L. Tits. A measure of worst-case $\mathcal{H}_\infty$ performance and of largest unacceptable uncertainty. *Syst. Contr. Lett.*, 18(6):409–421, 1992.

T. T. Georgiou and M. C. Smith. Optimal robustness in the gap metric. *IEEE Trans. Automat. Contr.*, 35(6):673–686, 1990.

M. Gevers. Towards a joint design of identification and control ? In H. L. Trentelman and J. C. Willems, editors, *Essays on Control : Perspectives in the Theory and its Applications*, chapter 5, pages 111–151. Birkhäuser, Boston, MA, USA, 1993. ISBN 0-8176-3670-6.

M. Gevers. Identification for control: From the early achievements to the revival of experiment design. *Eur. J. Contr.*, 11(4-5):1–18, 2005.

R. van Herpen, T. Oomen, and O. Bosgra. A robust-control-relevant perspective on model order selection. In *Proc. 2011 Americ. Contr. Conf.*, pages 1224–1229, San Francisco, CA, USA, 2011.

H. Hjalmarsson. From experiment design to closed-loop control. *Automatica*, 41:393–438, 2005.

M. Jung, K. Glover, and U. Christen. Comparison of uncertainty parameterisations for $\mathcal{H}_\infty$ robust control of turbocharged diesel engines. *Contr. Eng. Prac.*, 13(1):15–25, 2005.

D. C. McFarlane and K. Glover. *Robust Controller Design Using Normalized Coprime Factor Plant Descriptions*, volume 138 of *LNCIS*. Springer-Verlag, Berlin, Germany, 1990.

S. van der Meulen, B. de Jager, F. Veldpaus, E. van der Noll, F. van der Sluis, and M. Steinbuch. Improving continuously variable transmission efficiency with extremum seeking control. *IEEE Trans. Contr. Syst. Techn.*, DOI 10.1109/TCST.2011.2160980, 2012.

T. Oomen and O. Bosgra. Well-posed model uncertainty estimation by design of validation experiments. In *15th IFAC Symp. Sys. Id.*, pages 1199–1204, Saint-Malo, France, 2009.

T. Oomen and O. Bosgra. System identification for achieving robust performance. *Accepted for publication in Automatica*, 2012.

T. Oomen, S. Quist, R. van Herpen, and O. Bosgra. Identification and visualization of robust-control-relevant model sets with application to an industrial wafer stage. In *Proc. 49th Conf. Dec. Contr.*, pages 5530–5535, Atlanta, GA, USA, 2010a.

T. Oomen, S. van der Meulen, O. Bosgra, M. Steinbuch, and J. Elfring. A robust-control-relevant model validation approach for continuously variable transmission control. In *Proc. 2010 Americ. Contr. Conf.*, pages 3518–3523, Baltimore, MD, USA, 2010b.

R. J. P. Schrama. Accurate identification for control: The necessity of an iterative scheme. *IEEE Trans. Automat. Contr.*, 37(7):991–994, 1992.

S. Skogestad and I. Postlethwaite. *Multivariable Feedback Control: Analysis and Design*. John Wiley & Sons, West Sussex, UK, second edition, 2005.

R. S. Smith and J. C. Doyle. Model validation: A connection between robust control and identification. *IEEE Trans. Automat. Contr.*, 37(7):942–952, 1992.

O. Toker and J. Chen. On computational complexity of invalidating structured uncertainty models. *Syst. Contr. Lett.*, 33(3):199–207, 1998.

G. Vinnicombe. *Uncertainty and Feedback: $\mathcal{H}_\infty$ loop-shaping and the ν-gap metric*. Imperial College Press, London, UK, 2001.

M. van de Wal, G. van Baars, F. Sperling, and O. Bosgra. Multivariable $\mathcal{H}_\infty/\mu$ feedback control design for high-precision wafer stage motion. *Contr. Eng. Prac.*, 10(7):739–755, 2002.

K. Zhou, J. C. Doyle, and K. Glover. *Robust and Optimal Control*. Prentice Hall, Upper Saddle River, NJ, USA, 1996.